AGENCY FOR INTERNATIONAL DEVELOPMENT
WASHINGTON, D. C. 20523

BIBLIOGRAPHIC INPUT SHEET

FOR AID USE ONLY
0104

1. SUBJECT CLASSIFICATION

A. PRIMARY
Agriculture — AP10-0000-G518

B. SECONDARY
Water resources and management--Colombia

2. TITLE AND SUBTITLE
Hybrid computer simulation of groundwater regimes

3. AUTHOR(S)
Wang,Bi-huei; Riley,J.P.

4. DOCUMENT DATE	5. NUMBER OF PAGES	6. ARC NUMBER
1971	32p.	ARC 338.91.W246

7. REFERENCE ORGANIZATION NAME AND ADDRESS
Utah State

8. SUPPLEMENTARY NOTES *(Sponsoring Organization, Publishers, Availability)*
(Presented at Am.Geophysical Union,fall annual meeting,San Francisco)

9. ABSTRACT

10. CONTROL NUMBER	11. PRICE OF DOCUMENT
PN-RAA-053	

12. DESCRIPTORS
Atlantico 3 Project
Colombia
Computer programs
Ground water

13. PROJECT NUMBER

14. CONTRACT NUMBER
CSD-2167 Res.

15. TYPE OF DOCUMENT

AID 590-1 (4-74)

2167

ABSTRACT

HYBRID COMPUTER SIMULATION OF GROUNDWATER REGIMES[1]

by

Bi-Huei Wang[2] and J. Paul Riley[3]

A computer model is described which simulates the response of the groundwater table to various rates of input and abstraction. The model consists of two linked submodels each of which simulates the surface and the groundwater system, respectively. The surface submodel consists of mathematical expressions for the various processes of evapotranspiration, surface runoff, infiltration, and percolation which are functions of the soil characteristics, crop-pattern, and topography. Basic input data are precipitation, temperature, and irrigation and drainage rates. The groundwater submodel simulates the fluctuation of the groundwater table as a function of effective percolation and aquifer characteristics and is described by a two-dimensional second order partial differential equation of parabolic type with Dirichlet type boundary conditions. The partial differential equation describing the groundwater system is solved by the numerical alternating direction method. The application of the general model to a particular area is described. A grid is superimposed upon the study area and at each grid point the effective percolation rate to (or withdrawal from) the groundwater table is simulated. Calibration is accomplished by using a period of reliable data to identify the model parameters. Groundwater responses under various agricultural management alternatives of cropping and irrigation are predicted.

---

[1]The work described herein was financed by the U. S. Agency for International Development under Constract No. AID/csd 2167. The paper was prepared for presentation at the Fall Annual Meeting of the American Geophysical Union in San Francisco, December 1971.

---

[2]Research Assistant Professor, College of Engineering, Utah Water Research Laboratory, Utah State University, Logan, Utah.

[3]Professor, College of Engineering, Utah Water Research Laboratory, Utah State University, Logan, Utah.

TABLE OF CONTENTS

Page

Introduction 1

Theoretical Consideration 3

The surface and subsurface subsystem 3
The groundwater system 8

Computer Implementation 14

Management Study 17

Summary and Discussion 20

References 28

Appendix 1 30

LIST OF FIGURES

Figure 1 2
Figure 2 4
Figure 3 7
Figure 4 7
Figure 5 12
Figure 6 15
Figure 7 19
Figure 8 21
Figure 9 22
Figure 10 23
Figure 11 24
Figure 12 25
Figure 13 26

LIST OF TABLES

Table 1 18

Introduction

Over-irrigation of low-lying flat lands often results in excessive build-up of groundwater tables which are undesirable in many cases. The purpose of this study has been to investigate the response of the groundwater table to the rates of water supply and drainage for an area near the coast of northwestern Colombia, South America, and thereby to provide information for the optimal design of irrigation and drainage systems for the area.

The study area includes approximately 300 km^2 and has as its boundaries the Magdalena River on the east, the Canal del Dique on the south, the Guajaro Reservoir on the west, and a hilly region in the north as shown in Figure 1. In general, the land surface slopes slightly from the boundaries toward the center of the area, and there is no surface drainage from the area. Vegetative cover is largely native at the present time, but will be replaced by agricultural crops as a result of extensive agricultural development being planned.

The groundwater storage beneath this area is recharged by lateral groundwater in flows from the river, canal, reservoir, and mountains to the north, and by deep percolation from the land surface during the wet season when precipitation exceeds evapotranspiration. Extractions from the groundwater storage occur mainly as transpiration by the native phreatophytic vegetation. This transpiration by phreatophytes together

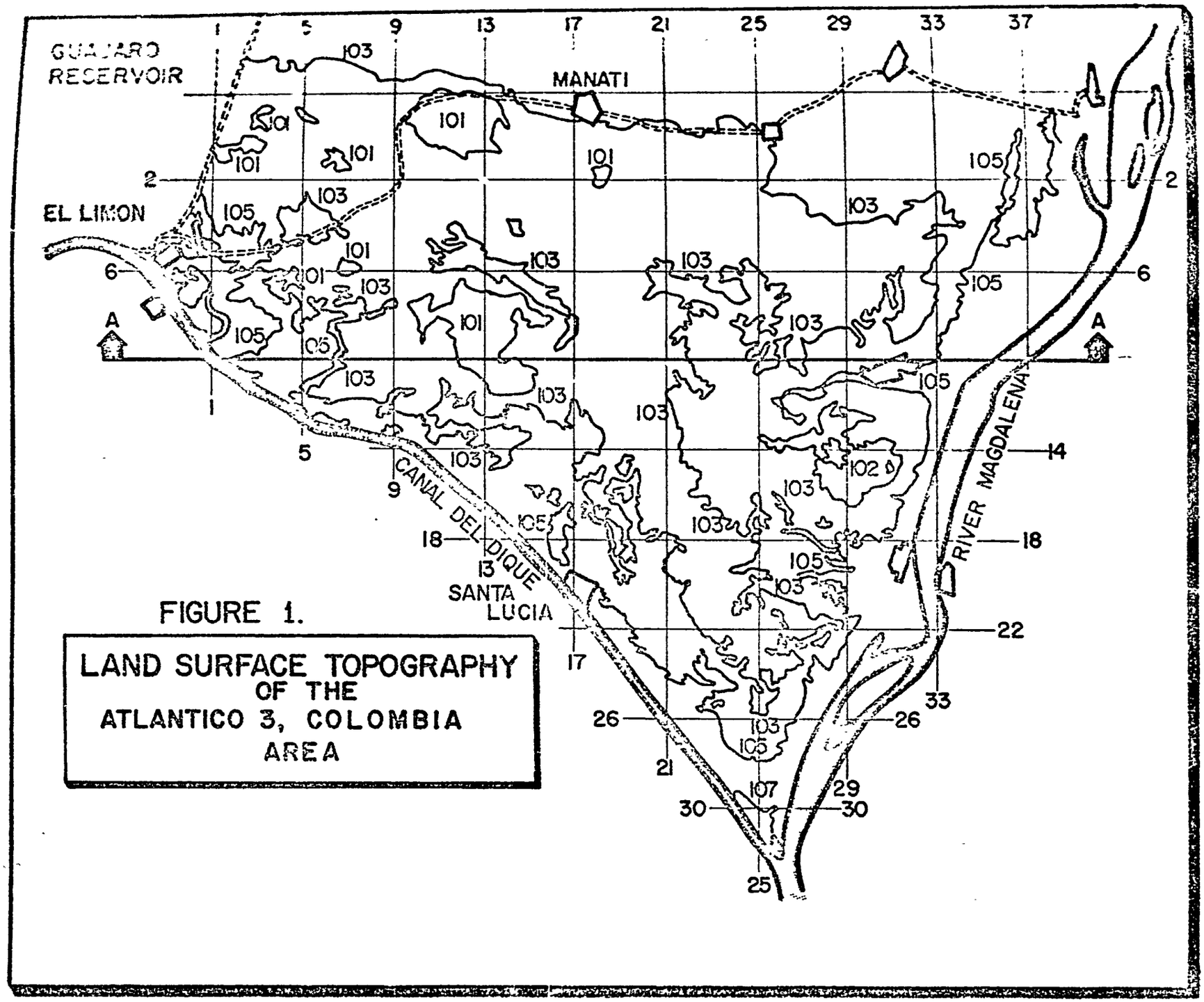

FIGURE 1.

LAND SURFACE TOPOGRAPHY
OF THE
ATLANTICO 3, COLOMBIA
AREA

with evaporation from the soil surface maintains the groundwater surface at an average depth of approximately 10 meters. Substitution of these native phreatophytes by shallow rooted agricultural crops will undoubtedly reduce extraction from the groundwater storage and, therefore, cause the groundwater table to rise gradually. Furthermore, cultivation of agricultural crops requires irrigation, and the excessive irrigation waters percolating downward will also accelerate the rise of the groundwater table. The response of the groundwater table to the reduction of native phreatophytes and application of irrigation and drainage systems, therefore, needs to be studied in the planning of agricultural activities for the area.

Theoretical Consideration

Attempts to describe the flow of water in natural soils often result in a three-dimensional partial differential equation of the parabolic type which is extremely difficult to solve. The present study, therefore, in attempting to simplify the problem, subdivided the system under consideration into two subsystems--the surface and subsurface subsystem and the groundwater subsystem--as discussed in the following paragraphs.

The surface and subsurface subsystem. This subsystem considers the water supply, drainage, evapotranspiration, infiltration, soil moisture storage, and percolation processes linked by the equation of continuity. A schematic diagram of the subsystem is shown as Figure 2. Definitions of the component processes in the subsystem are as follows.

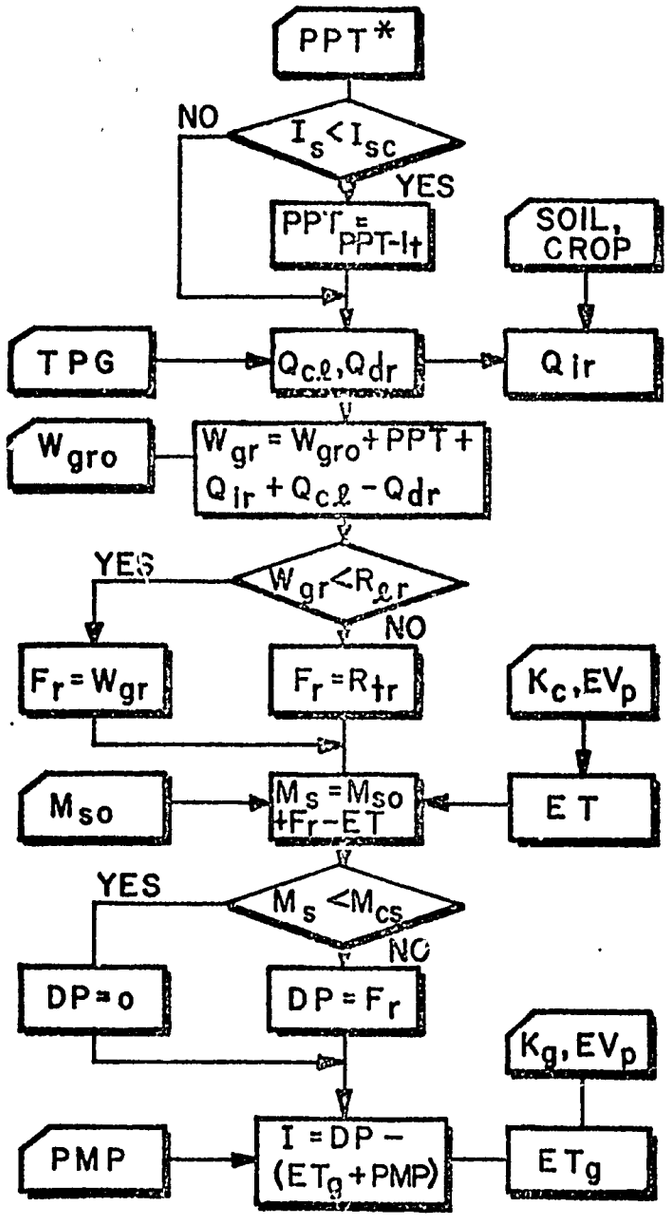

* See Appendix 1 for notation

Figure 2. Schematic Diagram of the Surface and Subsurface Subsystem.

Water Supply: Total water supplied to the ground surface is defined by the sum of precipitation and irrigation which is a function of soil and crop pattern.

Drainage: When the rate of water supply exceeds the rate of infiltration, the excess water begins to move along the ground surface. With respect to a particular point in the area, the rate of drainage at any time may be positive or negative depending on the topography. A topographic parameter which indicates the drainage or collection of water as introduced to characterize the movement of the excess water.

Evapotranspiration: There are numerous methods available for estimating evapotranspiration. As the result of a careful survey of these methods in the light of available data, the following method was considered appropriate for the present study.

$$ET_p = K\,EV_p \qquad (1)$$

in which

ET_p = rate of potential evapotranspiration

EV_p = rate of class-A pan evaporation

K = an experimentally determined coefficient which is dependent upon crop species and growing stage

The actual evaporation is usually less than the potential evapotranspiration when soil moisture is limited. Many approaches have been proposed by different investigators to relate the rate of actual and

potential evapotranspiration to the soil moisture as shown in Figure 3 (Hagen, Haise, and Edminster (1967), page 558).

The relationship described by the line F was accepted for the present study. In mathematical form, this relationship can be written as

$$ET_a = ET_p, \quad M_s \geq M_{es}$$

$$ET_a = \frac{M_s - M_{wp}}{M_{es} - M_{wp}} \quad (ET_p), \quad M_{wp} \leq M_s < M_{es}$$

$$ET_a = 0, \quad M_s < M_{wp} \qquad \ldots\ldots\ldots\ldots \qquad (2)$$

Infiltration, Soil Moisture, and Percolation: Infiltration is the passage of water through the ground surface into the soil and percolation is the downward movement of infiltrated water through the soil. There are numerous expressions to predict infiltration and percolation. The Darcian-based equation which describes vertical flow of water in a partly saturated porous medium constitutes a sound model for simulating the processes, but for the area under study, sufficient data were not available to properly define the hydraulic conductivity vs. soil moisture and the moisture diffusivity vs. soil moisture relationships involved in the equation. A less sophisticated but practical method used by Riley, Chadwick, and Bagley (1966) was, therefore, accepted for the present study. This method is as follows:

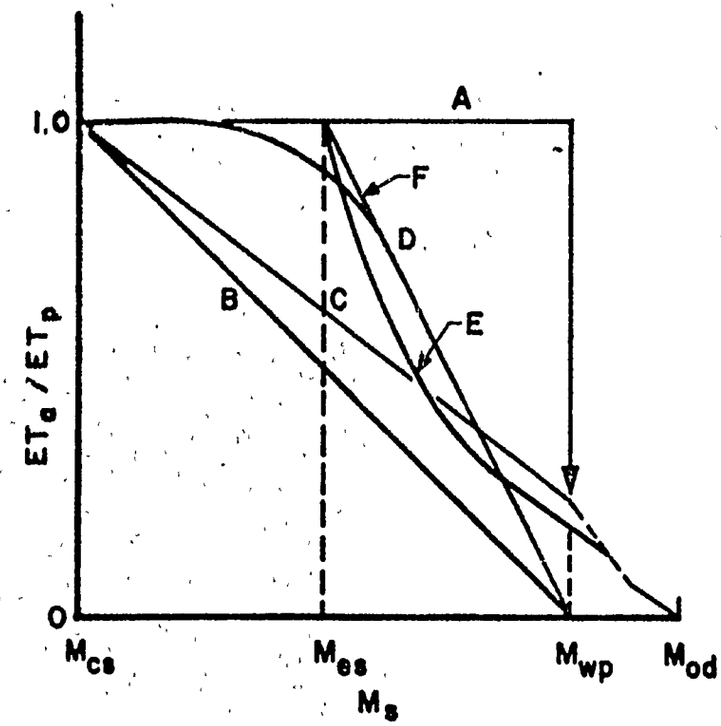

A. Veihmeyer and Hendrickson (1955)

B. Thornthwaite and Mather (1955)

C. Havens (1956)

D. Pierce (1958)

E. Penman (1949) and others

M_s Actual Soil Moisture

M_{cs} Soil Moisture Holding Capacity

M_{es} Minimum Soil Moisture for Evaporation at Potential Rate

M_{wp} Permanent Wilting Point

M_{od} Oven Dry Soil Moisture

Figure 3. Proposed relations of ET_a / ET_p vs M_s

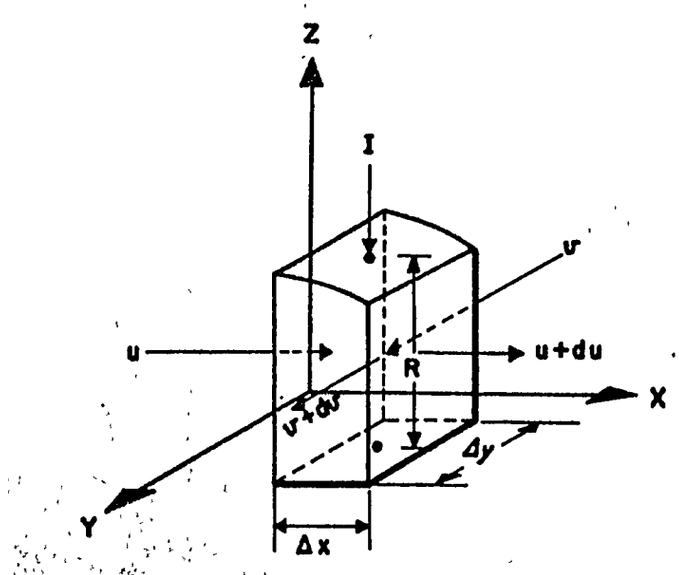

Figure 4. An Element Volume of the Aquifier.

$$F_r = W_{gr} \ , \quad W_{gr} < R_{tr}$$

$$F_r = R_{tr} \ , \quad W_{gr} \geq R_{tr} \tag{3}$$

in which

F_r is the monthly infiltration, R_{tr} is a threshold value with all available water in excess of this quantity being assumed to comprise surface runoff for the month, and W_{gr} is the quantity of water available at the soil surface during the month.

Based on this method, it is assumed that the infiltrated water satisfies the soil moisture deficit before any percolation occurs. When the soil moisture reaches field capacity, additional infiltrated water percolates to groundwater storage.

<u>The groundwater system.</u> Considering a three-dimensional element of a homogeneous isotropic unconfined aquifer as shown in Figure 4 and making the Dupuit assumptions, Darcy's law for the groundwater flow in the x and y directions is given by

$$u = -k\frac{\partial h}{\partial x} \tag{4}$$

and

$$v = -k\frac{\partial h}{\partial y} \tag{5}$$

in which

u, v = the seepage velocity in the x and y direction, respectively

k = hydraulic conductivity of the soil

h = depth from the impervious layer to the groundwater surface

By combining Equations (4) and (5) with the equation of continuity, the following equation results

$$\frac{\partial^2 h^2}{\partial x^2} + \frac{\partial^2 h^2}{\partial y^2} + \frac{2I}{k} = \frac{\epsilon}{T}\frac{\partial h^2}{\partial t} \quad . \quad . \quad . \quad . \quad . \quad . \quad . \quad (6)$$

in which

I = rate of net vertical recharge per unit area

T = transmissibility of the aquifer

ϵ = effective porosity (or specific yield) of the aquifer

Expanding Equation (6) and neglecting the terms $(\frac{\partial h}{\partial x})^2$ and $(\frac{\partial h}{\partial y})^2$, the following equation is obtained. The justification for neglecting $(\frac{\partial h}{\partial x})^2$ and $(\frac{\partial h}{\partial y})^2$ was examined by comparing the numerical values of different terms in the expanded equation based on the available groundwater table maps for the area.

$$\frac{\partial^2 h}{\partial x^2} + \frac{\partial^2 h}{\partial y^2} + \frac{I}{T} = \frac{\epsilon}{T}\frac{\partial h}{\partial t} \quad . \quad . \quad . \quad . \quad . \quad . \quad . \quad (7)$$

This is a linear partial differential equation of parabolic type. To solve the equation, the numerical alternating direction method discussed by Peaceman and Rochford (1955) was considered appropriate. The method, as for other difference methods, approximates the partial

differential equation of the problem and its boundary conditions by equivalent differences except that finite difference operators are applied twice for each time step. The difference equation for the first half-time step is implicit only in one direction and that for the second half-time step is implicit only in the other direction. In difference form, Equation (7) can be written as

$$\frac{h_{i,j}^{*} - h_{i,j}^{n}}{\Delta t/2} = \frac{T}{\epsilon}\left[\delta_x^2 h_{i,j}^{*} + \delta_y^2 h_{i,j}^{n} + \frac{I_{i,j}}{T}\right] \quad . \quad . \quad (8a)$$

$$\frac{h_{i,j}^{n+1} - h_{i,j}^{*}}{\Delta t/2} = \frac{T}{\epsilon}\left[\delta_x^2 h_{i,j}^{*} + \delta_y^2 h_{i,j}^{n+1} + \frac{I_{i,j}}{T}\right] \quad . \quad (8b)$$

in which the δ's denote second central difference operators. Written out in full and rearranged, with $\Delta x = \Delta y$, these equations become:

$$-\frac{T\lambda}{2\epsilon} h_{i-1,j}^{*} + \left(1 + \frac{T\lambda}{\epsilon}\right) h_{i,j}^{*} - \frac{T\lambda}{2\epsilon} h_{i+1,j}^{*}$$

$$= \frac{T\lambda}{2\epsilon} h_{i,j-1}^{n} + \left(1 - \frac{T\lambda}{\epsilon}\right) h_{i,j}^{n} + \frac{T\lambda}{2\epsilon} h_{i,j+1}^{n} + \frac{\Delta t}{2\epsilon} I_{i,j}$$

$$. \quad . \quad . \quad . \quad . \quad . \quad . \quad (9a)$$

$$-\frac{T\lambda}{2\epsilon} h_{i,j-1}^{n+1} + \left(1 + \frac{T\lambda}{\epsilon}\right) h_{i,j}^{n+1} - \frac{T\lambda}{2\epsilon} h_{i,j+1}^{n+1}$$

$$= \frac{T\lambda}{2\epsilon} h_{i-1,j}^{*} + \left(1 - \frac{T\lambda}{\epsilon}\right) h_{i,j}^{*} + \frac{T\lambda}{2\epsilon} h_{i+1,j}^{*} + \frac{\Delta t}{2\epsilon} I_{i,j}$$

$$. \quad . \quad . \quad . \quad . \quad . \quad . \quad (9b)$$

in which $\lambda = \Delta t/(\Delta x)^2$

Incorporating boundary conditions, with irregular boundaries as shown in Figure 5(a) through 5(d), Equation (9a) becomes

$$(1 + \frac{T\lambda}{\epsilon p}) h_{IB,j}^{*} - \frac{T\lambda}{\epsilon(1+p)} h_{IB+1,j}^{*} = \frac{T\lambda}{\epsilon p(1+p)} h_{P}^{*}$$

$$+ \frac{T\lambda}{\epsilon q(1+q)} h_{Q}^{n} + (1 - \frac{T\lambda}{\epsilon q}) h_{IB,j}^{n} + \frac{T\lambda}{\epsilon(1+q)} h_{IB,j\pm1}^{n}$$

$$+ \frac{\Delta t}{2\epsilon} I_{IB,j} \qquad \text{for } i = IB \text{ and boundaries (a) and (b) respectively}$$

$$- \frac{T\lambda}{2\epsilon} h_{i-1,j}^{*} + (1 + \frac{T\lambda}{\epsilon}) h_{i,j}^{*} - \frac{T\lambda}{2\epsilon} h_{i+1,j}^{*} = \frac{T\lambda}{2c} h_{i,j-1}^{n}$$

$$+ (1 - \frac{T\lambda}{\epsilon}) h_{i,j}^{n} + \frac{T\lambda}{2\epsilon} h_{i,j+1}^{n} + \frac{\Delta t}{2\epsilon} I_{i,j} \qquad \text{for } IB < i < ID$$

$$- \frac{T\lambda}{\epsilon(1+r)} h_{ID-1,j}^{*} + (1 + \frac{T\lambda}{\epsilon r}) h_{ID,j}^{*} = \frac{T\lambda}{\epsilon r(1+r)} h_{R}^{*}$$

$$+ \frac{T\lambda}{\epsilon s(1+s)} h_{S}^{n} + (1 - \frac{T\lambda}{\epsilon s}) h_{ID,j}^{n} + \frac{T\lambda}{\epsilon(1+s)} h_{ID,j\pm1}^{n}$$

$$+ \frac{\Delta t}{2\epsilon} I_{ID,j} \qquad \text{for } i = ID \text{ and boundaries (c) and (d) respectively}$$

. . . . . (10a)

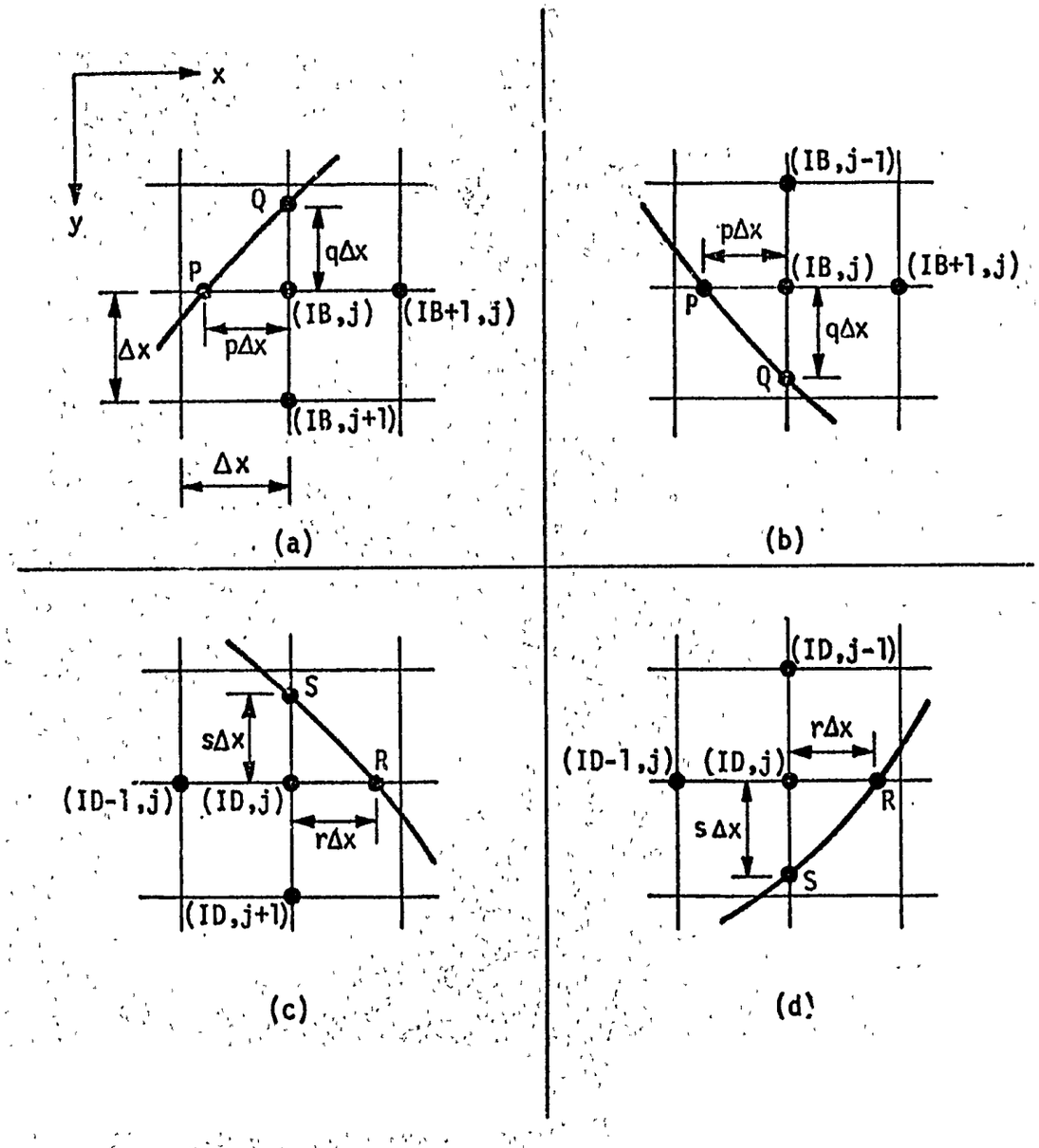

Figure 5. Irregular boundaries.

Similarly, Equation (9b) because

$$\left(1 + \frac{T\lambda}{\epsilon s}\right) h_{i,JB}^{n+1} - \frac{T\lambda}{\epsilon(1+s)} h_{i,JB+1}^{n+1} = \frac{T\lambda}{\epsilon s(1+s)} h_S^{n+1}$$

$$+ \frac{T\lambda}{\epsilon r(1+r)} h_R^{*} + \left(1 - \frac{T\lambda}{\epsilon r}\right) h_{i,JB}^{*} + \frac{T\lambda}{\epsilon(1+r)} h_{i-1,JB}^{*}$$

$$+ \frac{\Delta t}{2\epsilon} I_{i,JB} \qquad \text{for } j = JB \text{ and boundary (c)}$$

$$\left(1 + \frac{T\lambda}{\epsilon q}\right) h_{i,JB}^{n+1} - \frac{T\lambda}{\epsilon(1+q)} h_{i,JB+1}^{n+1} = \frac{T\lambda}{\epsilon q(1+q)} h_Q^{n+1}$$

$$+ \frac{T\lambda}{\epsilon p(1+p)} h_P^{*} + \left(1 - \frac{T\lambda}{\epsilon p}\right) h_{i,JB}^{*} + \frac{T\lambda}{\epsilon(1+p)} h_{i+1,JB}^{*}$$

$$+ \frac{\Delta t}{2\epsilon} I_{i,JB} \qquad \text{for } j = JB \text{ and boundary (a)}$$

$$-\frac{T\lambda}{2\epsilon} h_{i,j-1}^{n+1} + \left(1 + \frac{T\lambda}{\epsilon}\right) h_{i,j}^{n+1} - \frac{T\lambda}{2\epsilon} h_{i,j+1}^{n+1}$$

$$= \frac{T\lambda}{2\epsilon} h_{i-1,j}^{*} + \left(1 - \frac{T\lambda}{\epsilon}\right) h_{i,j}^{*} + \frac{T\lambda}{2\epsilon} h_{i+1,j}^{*} + \frac{\Delta t}{2\epsilon} I_{i,j}$$

$$\text{for } JB < j < JD$$

$$- \frac{T\lambda}{\epsilon(1+s)} h_{i,JD-1}^{n+1} + (1 + \frac{T\lambda}{\epsilon s}) h_{i,JD}^{n+1} = \frac{T\lambda}{\epsilon s(1+s)} h_S^{n+1}$$

$$+ \frac{T\lambda}{\epsilon r(1+r)} h_R^* + (1 - \frac{T\lambda}{\epsilon r}) h_{i,JD}^* + \frac{T\lambda}{\epsilon(1+r)} h_{i-1,JD}^*$$

$$+ \frac{\Delta t}{2\epsilon} I_{i,JD} \qquad \text{for } j = JD \text{ and boundary (d)}$$

$$- \frac{T\lambda}{\epsilon(1+q)} h_{i,JD-1}^{n+1} + (1 + \frac{T\lambda}{\epsilon q}) h_{i,JD}^{n+1} = \frac{T\lambda}{\epsilon q(1+q)} h_Q^{n+1}$$

$$+ \frac{T\lambda}{\epsilon p(1+p)} h_P^* + (1 - \frac{T\lambda}{\epsilon p}) h_{i,JD}^* + \frac{T\lambda}{\epsilon(1+p)} h_{i+1,JD}^*$$

$$+ \frac{\Delta t}{2\epsilon} I_{i,JD} \qquad \text{for } j = JD \text{ and boundary (b)} \tag{10b}$$

Computer Implementation

To examine the spatial variation as well as the time variation of the various processes in the system, the study area was represented by a square grid system with a grid spacing of 625 meters as shown in Figure 6. The mathematical models for both the surface and subsurface subsystem and the groundwater subsystem were then programmed on an EAI 590 hybrid computer for rapid operation.

For each of the grid points, the effective percolation to or abstraction from the groundwater during each time increment is simulated by the

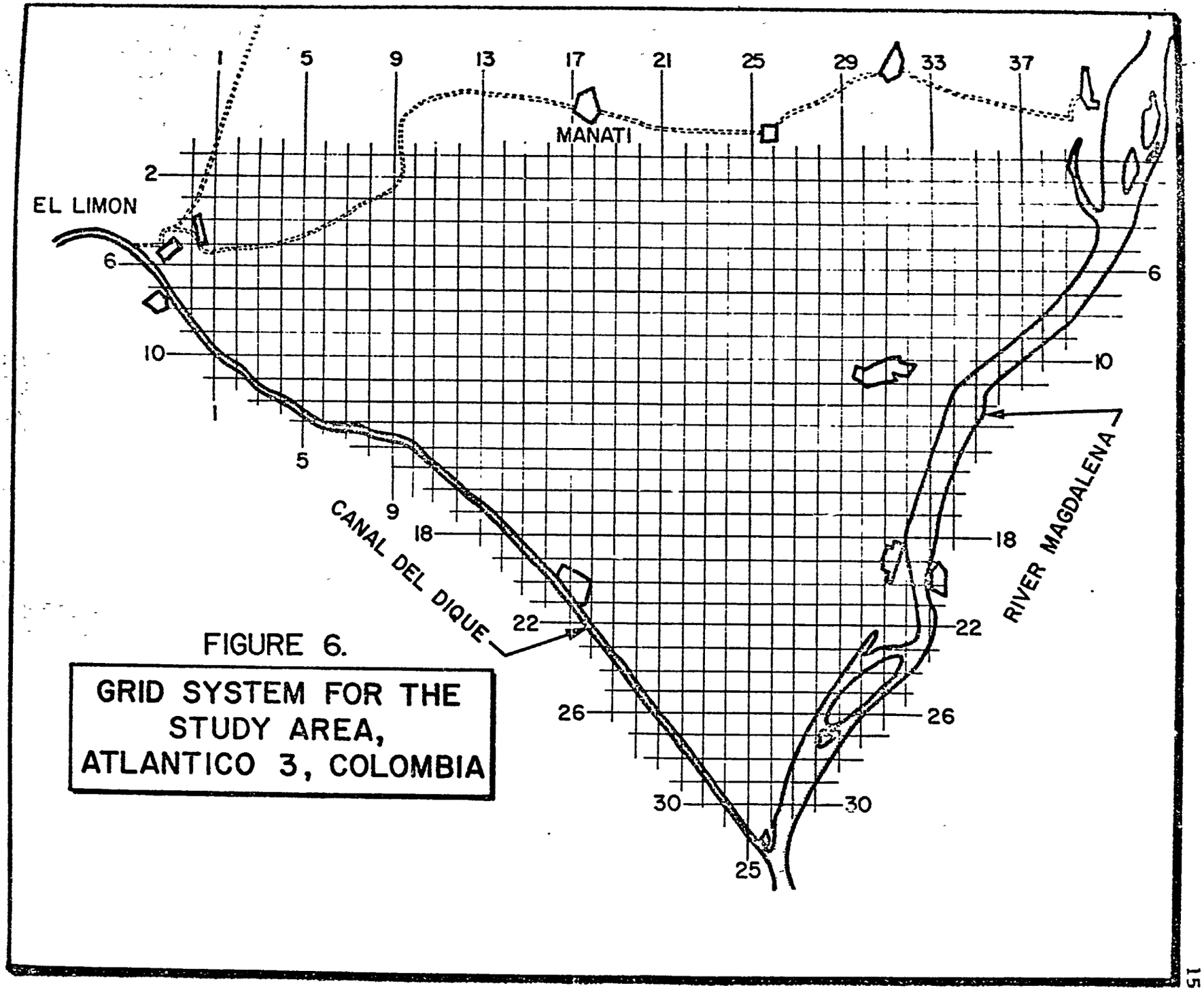

FIGURE 6.

GRID SYSTEM FOR THE STUDY AREA, ATLANTICO 3, COLOMBIA

surface and subsurface submodel as a function of the other processes in the subsystem. This simulated quantity (either positive or negative) at each grid point is then fed to the groundwater submodel to simulate the groundwater table fluctuations. The Dirichlet type boundary condition for the groundwater submodel was properly defined on the basis of the available data for Magdalena River, Canal del Dique, and Guajaro Reservoir that form the boundaries of the area.

The input data for the surface and subsurface submodel include precipitation, temperature, class-A pan evaporation, soil type and the corresponding crop pattern in terms of crop consumptive use coefficient and irrigation requirements, groundwater drainage rate, soil moisture holding capacity, initial soil moisture and swamp storage, phreatophyte and crop densities, and a topographic parameter discussed in a previous section. The output includes total evapotranspiration, groundwater extraction by phreatophytes, soil moisture, swamp storage, and effective percolation.

The input data for the groundwater submodel include, in addition to the effective percolation or abstractions generated by the surface and subsurface submodel, the initial water table, water table along the boundaries at different times, and the transmissibility and specific yield of the aquifer. The output of the submodel includes the height of groundwater surface above the impervious datum for each grid point at various times.

Both the surface and subsurface submodel and the groundwater submodel are calibrated over a period of time in which reliable observed data are available to identify the model parameters, particularly the transmissibility and specific yield of the groundwater aquifer.

Management Study

Based on the soil, land classification, and climatological data, certain land use patterns were assumed. These patterns and the corresponding consumptive use coefficients and irrigation requirements for each major class of soil in the area are shown by Table 1. The density of the native phreatophytes presently varies from 50 percent in the southeastern part of the area to 20 percent in the northwestern part of the area.

To investigate the response of the groundwater table to the reduction of native phreatophytes and the application of irrigation water, the model was first operated by assuming that the native phreatophytes are reduced by 50 percent, that crop patterns are as those in Table 1, and that no artificial subsurface drainage exists. Figure 7 shows the simulated groundwater table for the area under these conditions at the end of a period of six months. This figure suggests that under the conditions assumed the groundwater table would build up quickly to the crop root zone.

To estimate the rate of drainage required to prevent the groundwater table from excessive build-up, several drainage rates were assumed and the model was operated for each assumed rate. The assumption of an average drainage rate of 12 cm per month for the entire area

Table I. Crop-pattern, Crop-coefficients, & Irrigation for Different Soils.

SOIL GROUP	ITEM	CROP	CROP-PATTERN, WEIGHTED CROP-COEFFICIENT, AND IRRIGATION RATE											
			J	F	M	A	M	J	J	A	S	O	N	D
1	CROP PATTERN	CITRUS												
		PEANUTS												
		MAIZE												
	CROP COEFF.		.65	75	.55	.60	.45	.60	.75	.60	.60	.60	.60	.50
	IRR. RATE[1]		112	112	90	45	60	60	60	60	45	60	60	60
2	CROP PATTERN	COTTON												
		SORGHUM												
	CROP COEFF.		.70	.50	.20	.20	.30	.60	.90	.60	.40	.65	.90	.90
	IRR. RATE[1]		112	.90	0	0	45	60	60	60	60	60	90	112
3	CROP PATTERN	GRASSES												
	CROP COEFF.		.80	.80	.80	.80	.80	.80	.80	.80	.80	.80	.80	.80
	IRR. RATE[1]		90	90	90	75	60	60	60	60	60	60	75	90
4	CROP COEFF.	BARE SOIL	.15	.15	.15	.15	.20	.20	.20	.20	.20	.15	.15	.15
	IRR. RATE[1]		0	0	0	0	0	0	0	0	0	0	0	0

[1] In mm/month., irrigation efficiency =0.6

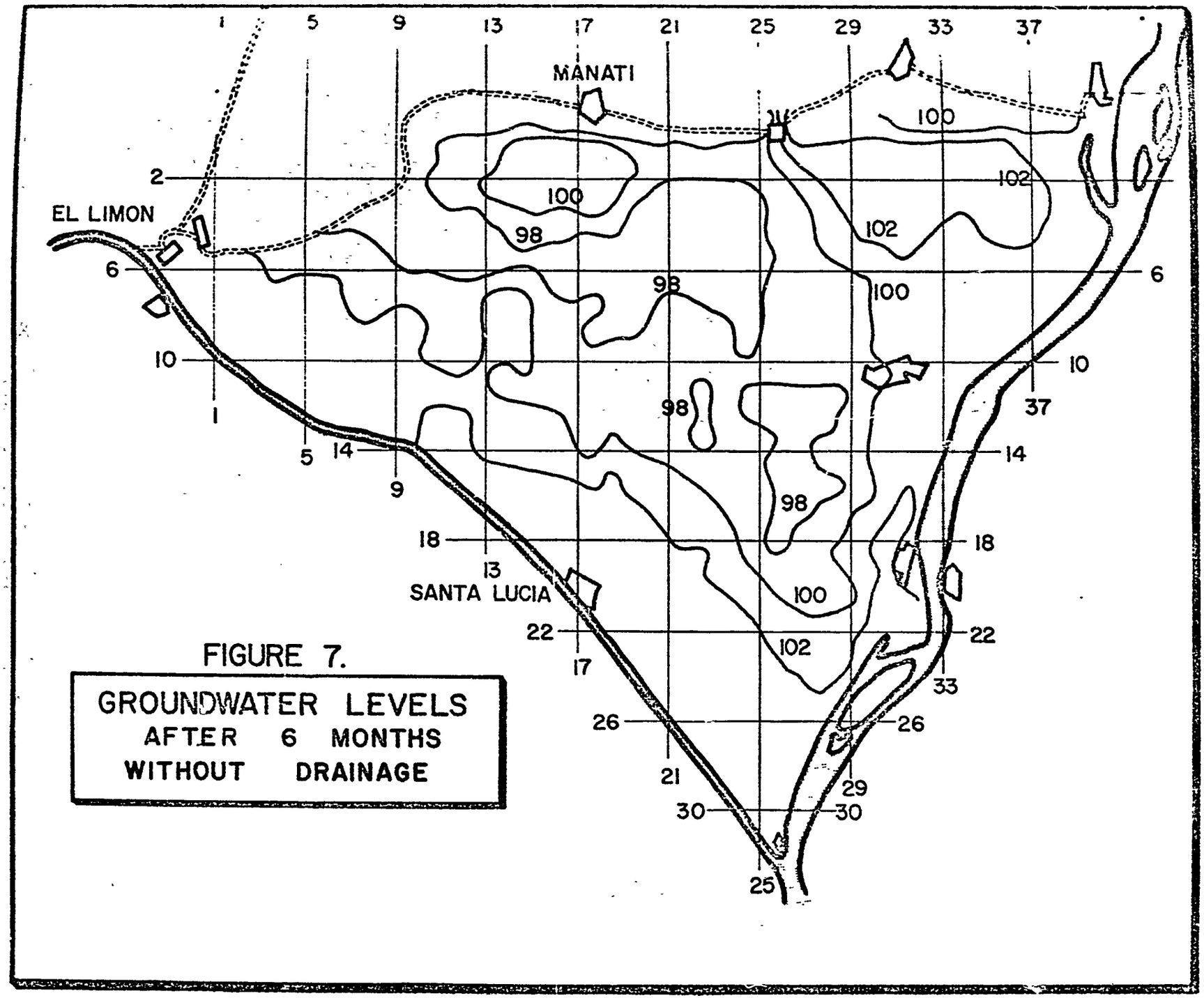

FIGURE 7.

GROUNDWATER LEVELS
AFTER 6 MONTHS
WITHOUT DRAINAGE

resulted in the groundwater table maps shown in Figures 8 through 12. The groundwater surface profile along section A-A in Figure 1 is shown by Figure 13. Under the assumed groundwater drainage rate, the water table apparently would tend to stabilize at a level which would be suitable for satisfactory crop growth.

Summary and Discussion

The response of the groundwater table of a low-lying flat land to the climate, crop pattern, irrigation, and drainage was investigated by a technique involving the computer simulation of the hydrologic and hydraulic processes. By means of the model responses of the system to various land use and water resource management alternatives were investigated. Results suggested that the model, which is generally applicable, is capable of establishment of a sound development plan for the study area. However, there was only three years of climatological records available at the time of the study, and on the basis of these short-period-records, climatological data were assumed for longer periods to study the long range behavior of the system. For a more reliable prediction of the system behavior, collection of the climatological data should be continued and analyzed for a longer period. At the time of the study, only one year of groundwater data were available in the form of groundwater table maps with a three-month time increment. These data were used to calibrate the model and to identify the model parameters, such as the transmissibility and specific yield of the groundwater aquifer. As additional groundwater data become available, further calibration of the model should be made to improve the reliability of the predictions.

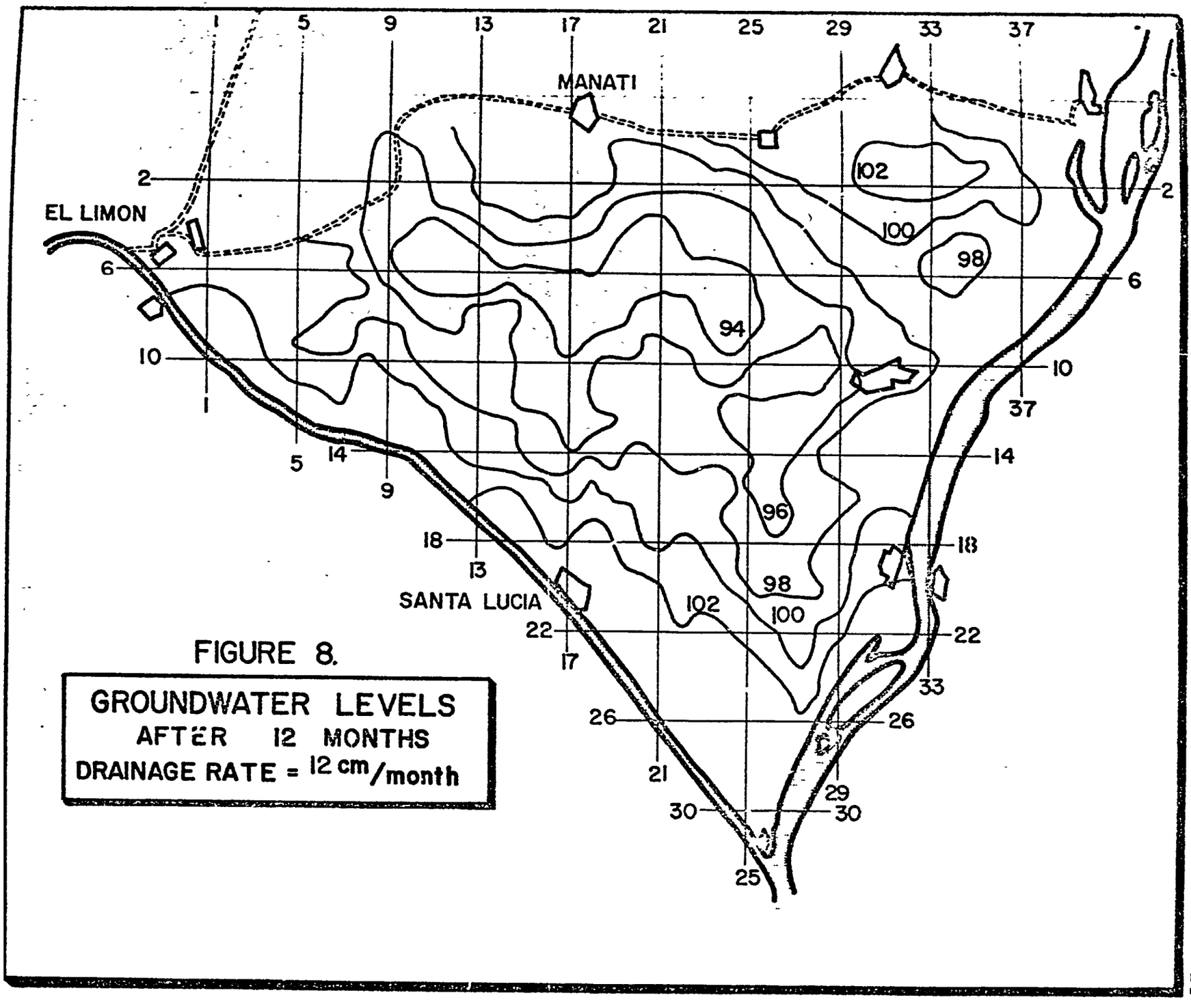

FIGURE 8.

GROUNDWATER LEVELS
AFTER 12 MONTHS
DRAINAGE RATE = 12 cm/month

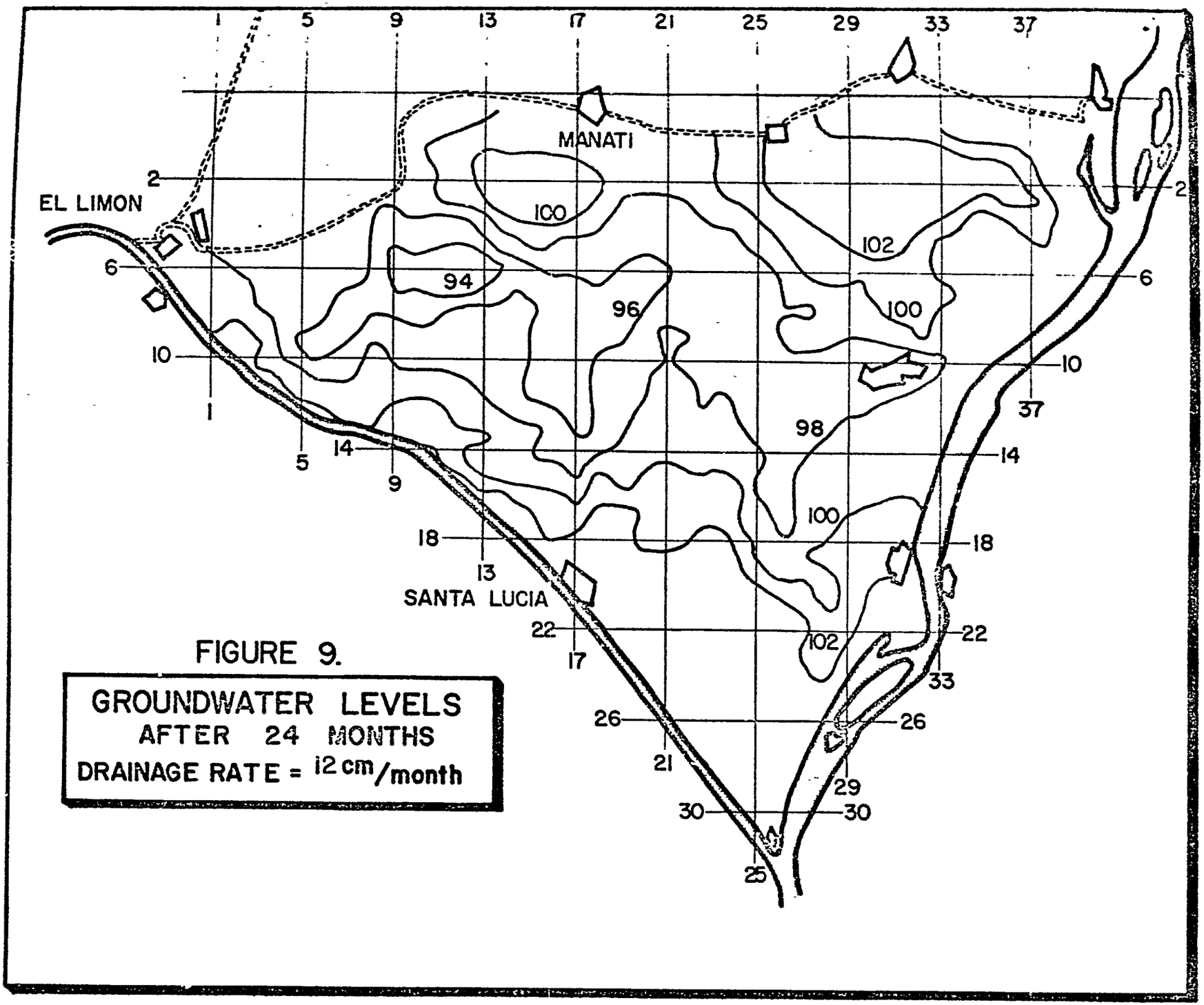

FIGURE 9.

GROUNDWATER LEVELS
AFTER 24 MONTHS
DRAINAGE RATE = 12 cm/month

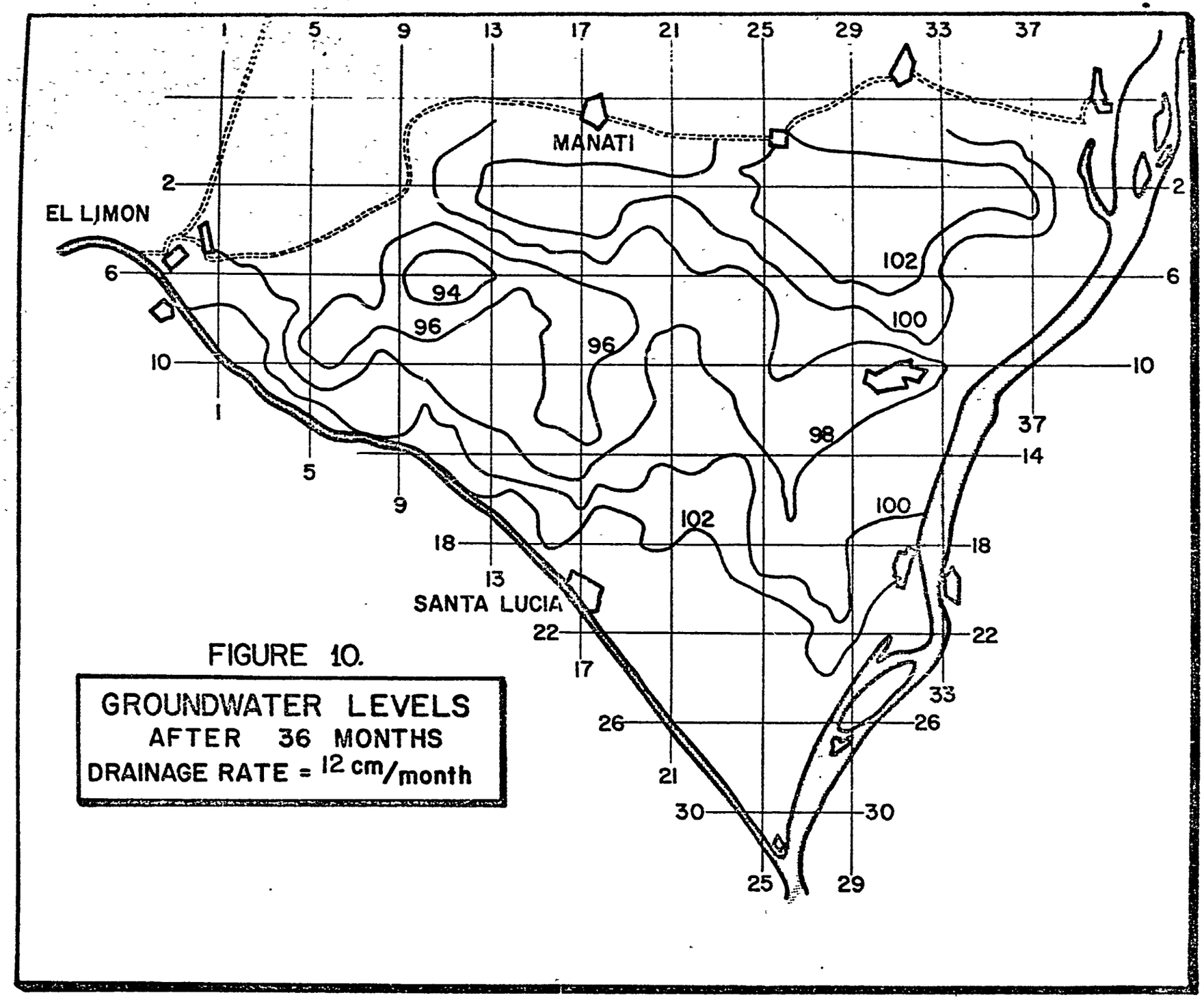

FIGURE 10.

GROUNDWATER LEVELS
AFTER 36 MONTHS
DRAINAGE RATE = 12 cm/month

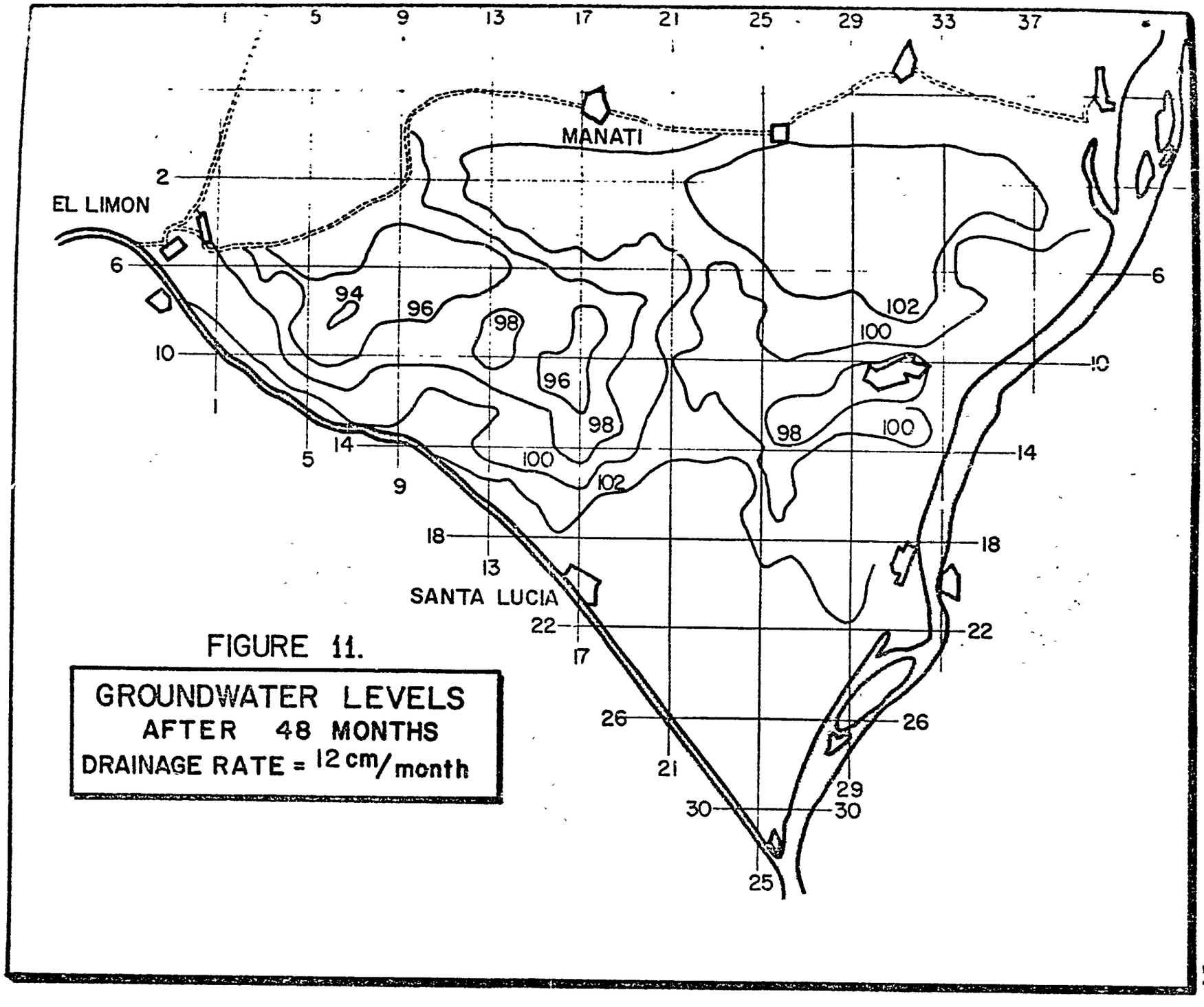

FIGURE 11.

GROUNDWATER LEVELS
AFTER 48 MONTHS
DRAINAGE RATE = 12 cm/month

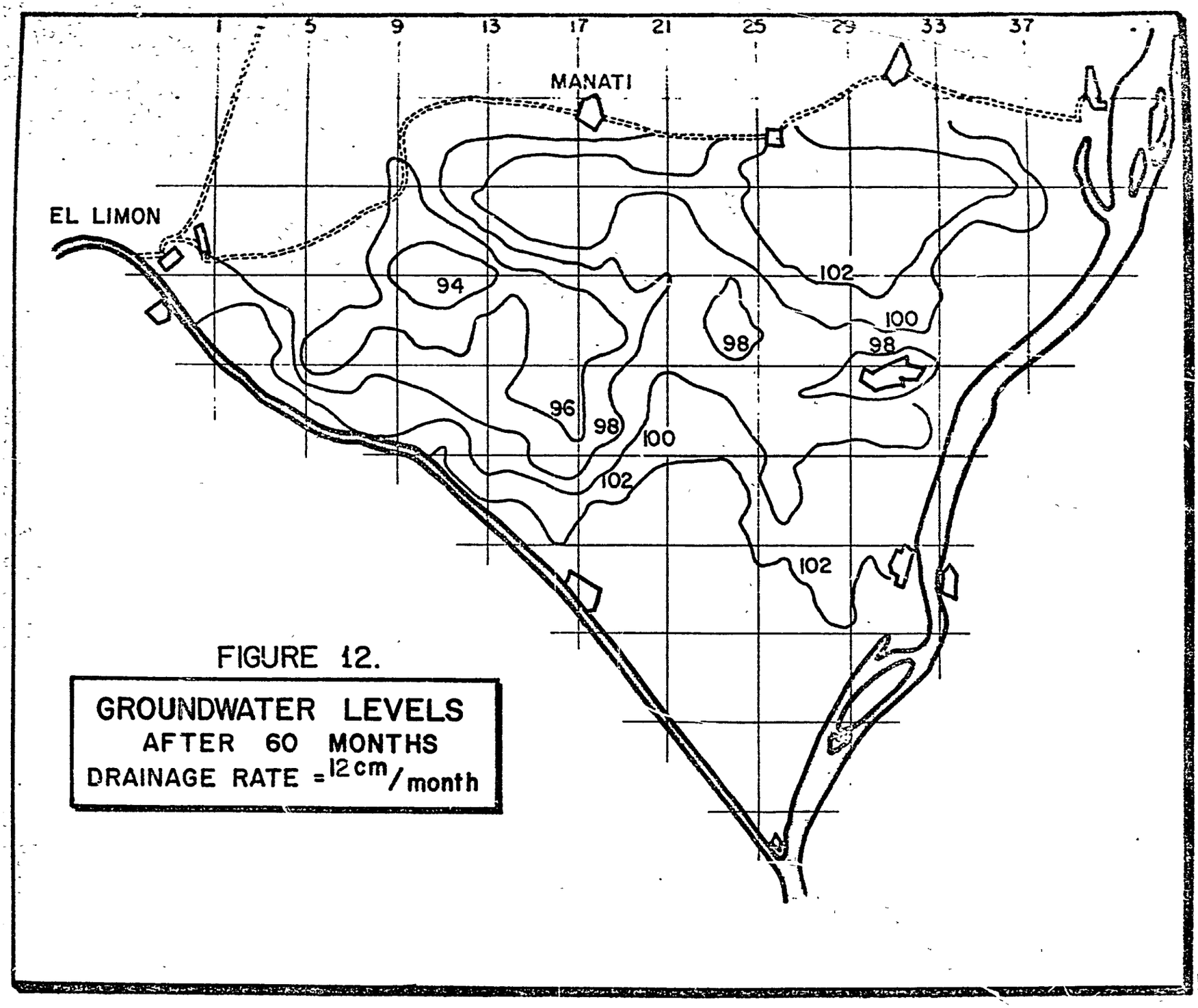

FIGURE 12.

GROUNDWATER LEVELS
AFTER 60 MONTHS
DRAINAGE RATE = 12 cm/month

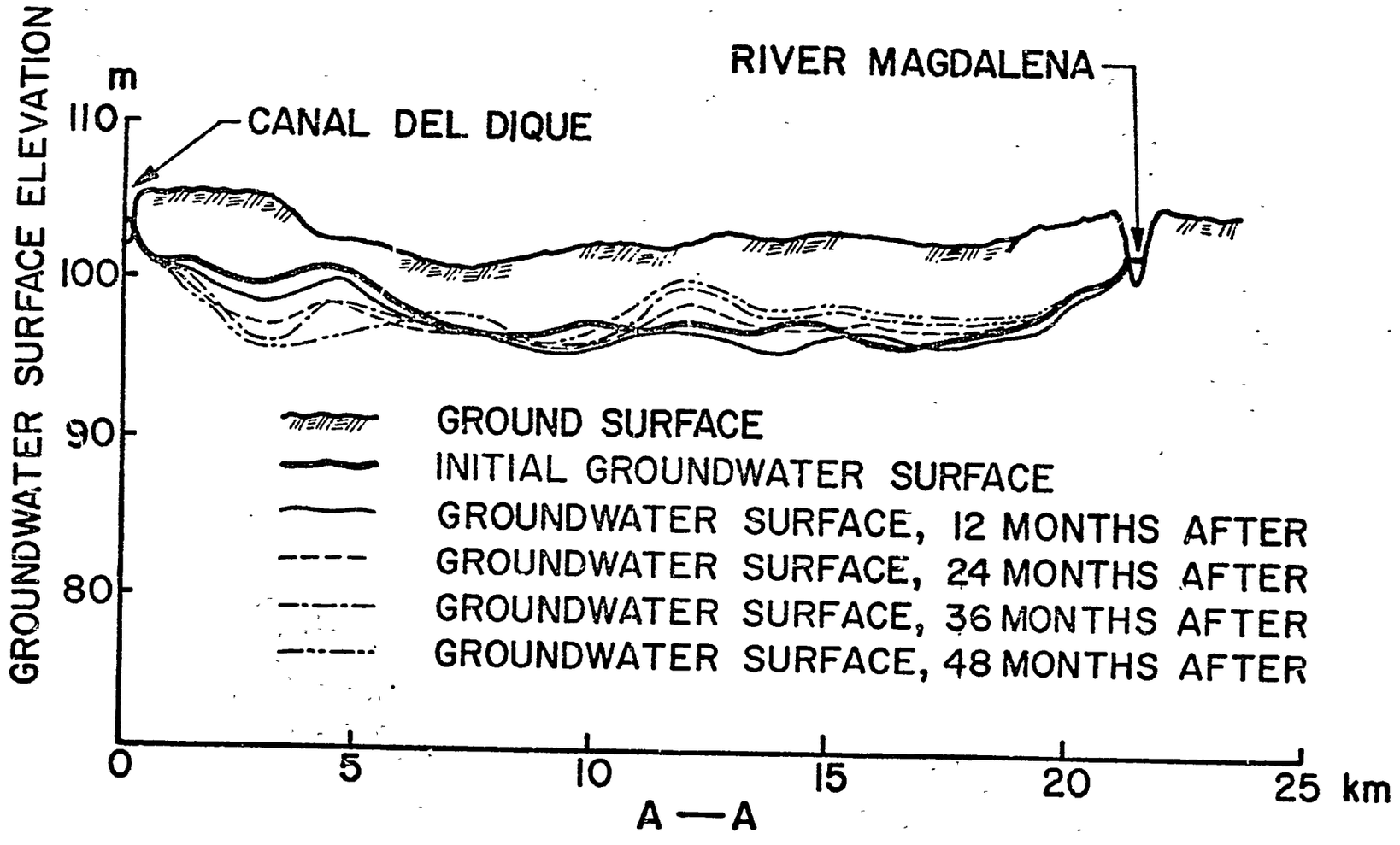

Figure 13. Groundwater Profile Along Section A—A, for Groundwater Drainage Rate of 10 mm/month.

In the initial management study reported here, a uniform rate of pumped drainage was assumed for the entire area and period of study. This assumption is likely not the most optimal pattern and schedule of drainage and the studies are now being made which include various combinations of gravity and pumped drainage systems.

In general, the computer model applied well to the particular problem under investigation. Because the model is based on fundamental concepts, it is not restricted by geographic limitations, and would apply equally well to many problems of similar nature. However, certain modifications would be needed for areas where homogeneous and isotropic groundwater aquifer conditions cannot be assumed.

References

Hagan, R. M., H. R. Haise, and P. W. Edminster. 1967. Irrigation of agricultural land. American Society of Agronomy, Publisher, Madison, Wisconsin.

Morris, W. J., N. W. Morgan, B. H. Wang, and J. P. Riley. 1970. Combined surface water-groundwater analysis of hydrological systems with the aid of the hybrid computer. Paper presented at the Sixth American Water Resources Conference, Las Vegas, Nevada.

Peaceman, D. W. and H. H. Rachford, Jr. 1955. The numerical solution of parabolic and elliptic differential equations. J. Soc. Indust. Appl. Math., 3, 28-41.

Riley, J. P., D. G. Chadwick, and J. M. Bagley. 1966. Application of electronic analog computer to solution of hydrologic and river-basin-planning problems: Utah simulation model II. Utah Water Research Laboratory, Utah State University, Logan, Utah.

Appendices

Appendix 1

Notation for Figure 2

DP = deep percolation

ET = evapotranspiration from unsaturated soil

ET_g = evapotranspiration from groundwater

EV_p = pan evaporation

F_r = infiltration

I = effective percolation

I_s = interception storage

I_{sc} = interception storage capacity

I_t = interception

K_c = crop consumptive use coefficient

K_g = phreatophyte consumptive use coefficient

M_{cs} = soil moisture holding capacity

M_s = soil moisture storage

M_{so} = initial soil moisture

PMP = pumping drainage

PPT = precipitation

Q_{cl} = surface water collection

Q_{dr} = surface drainage

R_{tr} = infiltration capacity

TPG = topographic parameter

W_{gr} = total water supply to ground surface

W_{gro} = initial water supply to ground surface